POAC'25
St. John's, Newfoundland and Labrador, Canada

Proceedings of the 28th International Conference on Port and Ocean Engineering under Arctic Conditions
Jul 13-17, 2025
St. John's, Newfoundland and Labrador
Canada

Ridge keel surcharge effect during an interaction with a cylindrical offshore structure

Jaakko Heinonen[1], Knut V. Høyland[2]
[1] VTT Technical Research Centre of Finland Ltd., Espoo, Finland
[2] The Norwegian University of Science and Technology (NTNU), Trondheim, Norway

ABSTRACT

In freezing sea areas, the major load for offshore structures is usually caused by drifting sea ice ridges, which consist of a sail above the water and a keel beneath the waterline. In first-year ridges, the keel consists of an upper refrozen or consolidated layer and unconsolidated rubble below. The major load contribution of an ice ridge is presented by the consolidated layer and the underlying keel.

Dolgopolov et al. (1975) published an analytical model for calculating the ridge load on a vertical pier. The model, adopted from soil mechanics, is based on passive earth pressure theory. It provides a ridge keel load for a vertically faced structure in an easy way using a limited number of input parameters. Due to its simplicity, the model has been adopted by ISO 19906 (2019).

When the ridge keel interacts with the vertically faced structure, part of the rubble – broken during the interaction – starts to accumulate in front of the structure. This means that the ice contact area against the structure increases. Dolgopolov et al. (1975) proposed to apply an increase in the keel thickness instead of the intact thickness of the ridge keel. This phenomenon is often called a surcharge effect.

In the original Dolgopolov model, the surcharge effect was considered by increasing the design keel thickness. The lower bound is equal to the original keel thickness, and the upper bound is equal to the original keel thickness plus half the diameter of the structure. However, this effect was not adopted by the ISO standard because it would result in extremely high ridge loads on very wide structures (80 m) (Kärna and Nykänen, 2004). For typical Baltic structures (mostly less than 10 m in width), the surcharge may be important, and non-conservative design loads can be estimated without it.

In this paper, we have carried out numerical simulations demonstrating both the keel deformations (surcharge) and the additional contact load regarding the surcharge. The simulations confirm that ice accumulates roughly as suggested by Dolgopolov et al. (1975), but the increase in horizontal force caused by the surcharge was minimal because the ridge material was weakened when broken (substantial softening).

KEY WORDS: Ridge keel; ice rubble; ridge load; offshore structure

INTRODUCTION

Dolgopolov *et al.* (1975) published an analytical model for calculating the ridge load on a vertical pier. The model, adopted from soil mechanics, is based on passive earth pressure theory. It provides design ridge loads for a vertically faced structure in an easy way using a limited number of input parameters. Based on its simplicity, the model has been adopted with small variations to ISO 19906 and other standards.

The keel load is calculated as

$$F_k = \mu_\phi h_k w \left(\frac{h_k \mu_\phi \gamma_e}{2} + 2c\right)\left(1 + \frac{h_k}{6w}\right) \quad (1)$$

Where h_k is the rubble depth (keel depth minus the consolidated layer) μ_ϕ is the passive pressure coefficient given as

$$\mu_\phi = \tan\left(45° + \frac{\phi}{2}\right) \quad (2)$$

ϕ is the angle of internal friction, c is the apparent keel cohesion (an average value over the keel volume), w is the width of the structure, γ_e is the effective buoyancy given as

$$\gamma_e = (1 - \eta)(\rho_w - \rho_i)g \quad (3)$$

where η is the keel porosity, ρ_w is the water density and ρ_i is the ice density.

When the ridge keel interacts with the vertically faced structure, part of the rubble broken during the interaction starts to accumulate in the front of the structure. This means that the ice contact area against the structure increases. Dolgopolov considers this as an increase in keel thickness compared to the intact ridge thickness. This phenomenon is often called a surcharge effect. The Dolgopolov model (1975) suggest a keel thickness h_{eff} as:

$$h_k \leq h_{eff} \leq h_k + \frac{w}{2} \quad (1)$$

Dolgopolov *et al.* (1975) state *that the design height of additional ice of triangular cross-section cannot exceed approximately half the pier width*. To our best understanding, this corresponds to triangular shapes of keel and surcharge with repose angles less than 45º.

However, this effect was not adopted into the ISO standard. One can conclude from Eq. 1 that the keel load is strongly proportional to the keel thickness squared. This means that for significant keel thicknesses, *e.g.* over 5 m, the surcharge effect has a significant influence on keel loads. Fig. 1 shows the influence of surcharge effect, when the diameter of the cylindrical structure is 4 and 10 m and the keel depth is 8 m. These represent reasonable dimensions for offshore wind turbines and ice conditions in the Baltic Sea. One can conclude that the surcharge effect is much higher when the structure is wide, *i.e.* the ratio between the diameter and ridge thickness is high. However, this effect was not adopted to the ISO standard because it would result in extremely high ridge loads on very wide structures often used for oil and gas platforms (width 80 m or even more). Palmer and Croasdale (2012) presented a semi-analytical model for ridge interaction with vertical structures that includes both passive local failure (similar to

Dolgopolov) and global failure (plug failure). The maximum ridge load should be taken as the minimum of the two. They also recommended a surcharge factor of less than 0.1.

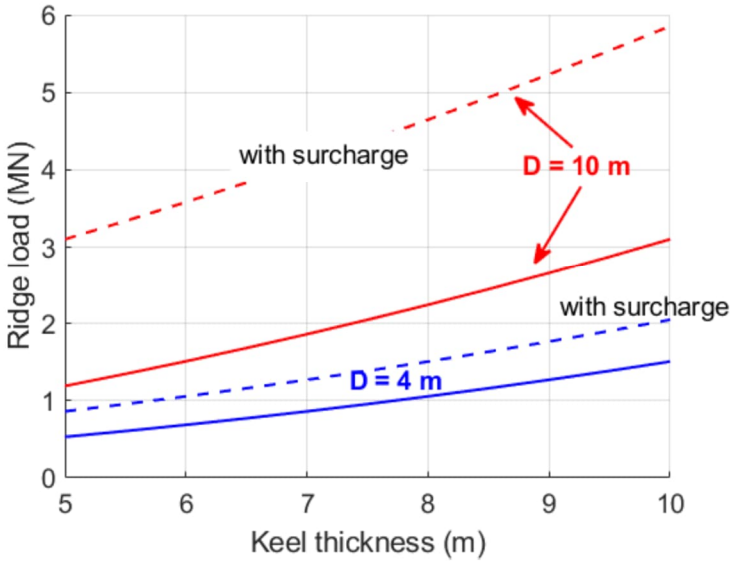

Figure 1. Ridge keel load on a cylindrical structure (diameter 4 m and 10 m) as a function of keel thickness calculated by Dolgopolov's model. Surcharge effect with a design keel thickness of $h_{eff} = h_k + w/2$ is demonstrated by dashed lines.

Ridge interaction with a cylindrical structure was earlier studied by Heinonen (2022), in which a 6 m wide structure penetrated into an 8 m thick ridge keel. Numerical simulations showed significant rubble accumulation in front of the structure. When the maximum load was reached, the keel thickness at the contact area of structure increased by 2.5 m, and the total rubble depth became 10.5 m. Based on Dolgopolov's upper bound of surcharge, which is half of the width of the structure, i.e. in this case 6 m /2 = 3m, the numerical simulation supports Dolgopolov's design keel thickness theorem well.

Serre and Liferov (2010) conducted numerical simulations to study the surcharge effect on a cylindrical structure with a diameter of 1 m. They observed that Dolgopolov's model without the surcharge (the ISO model) matches well with the numerical simulation, but only if the surcharge effect is removed from the numerical model. They concluded that the effect of surcharge on the keel load can be significant, especially for wide structures with poor ice-clearing capabilities and fairly deep and wide ridges. Serre and Liferov (2010) further concluded that the role of the material model of ice rubble and its parameters is crucial when simulating the rubble accumulation.

Ice ridge interaction with bottom-fixed conical (and cylindrical) structures was studied through model-scale experiments in the Aalto ice tank, as presented by Shestov *et al.* (2020), Salganik *et al.* (2021), Jiang *et al.* (2021, 2020) and Heinonen *et al.* (2021). The test set-up consisted of cameras below water level to provide the view and depth measurement of rubble pile accumulation in front of the structure and the side view of the rubble pile passing the structure. Based on underwater camera observations, the volume of accumulated ice mass in front of the

cylindrical structure was determined. Four test runs with a 0.35 m keel resulted in deformed keel thicknesses between 0.4 m and 0.75 m. These are somewhat in the range of design keel thickness according to Dolgopolov *et al.* (1975). As the diameter of the cylinder was 0.5 m, the range becomes from 0.35 m to 0.725 m.

The aim of this study was to carry out ridge-structure interaction simulations to gain more understanding about keel deformations on cylindrical structures and the load contribution of deformed keel (surcharge). The numerical simulation procedure was based on Coupled Eulerian-Lagrangian (CEL) framework in Abaqus/Explicit (Heinonen, 2022) with a user subroutine to describe the material model of ice rubble (Heinonen, 2004).

MATERIAL MODEL FOR ICE RUBBLE

For modeling the failure process in the ice rubble, a shear-cap failure criterion was earlier developed by the author (Heinonen, 2004). This model is suitable for numerical continuum-based finite element simulations. The main failure mechanisms modelled by the shear-cap model are the shear failure and compaction of ice rubble (see Figure 2). As in other frictional-cohesive material models, the main parameters to model the shear failure are the cohesion and friction angle. Post-failure behaviour is modelled by cohesive softening. Deformations in the failure process are modelled with an associative flow rule, which describes dilatation during the shear failure and compaction during the cap failure. Due to the porous nature of ice rubble, modelling of volumetric behaviour is essential. Volumetric change in the rubble is modelled using the cap hardening feature. More details about the material model are described in Heinonen (2004).

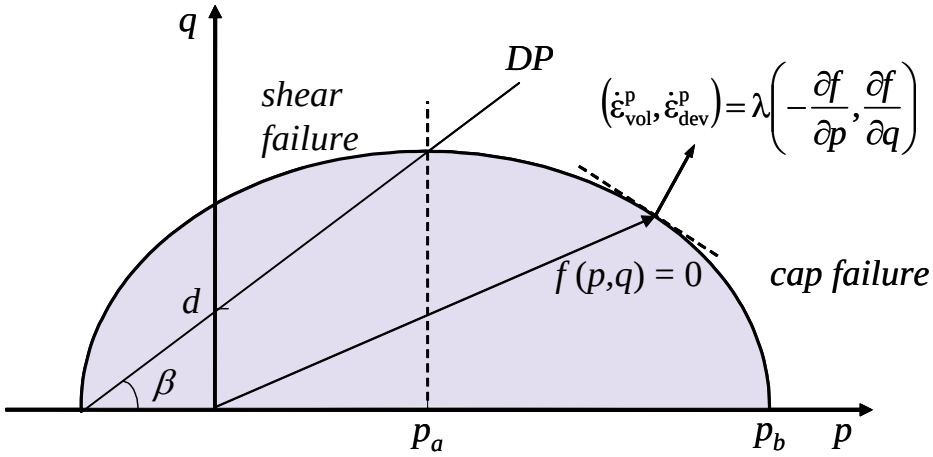

Figure 2. Shear-cap yield function in the meridian plane. p is the hydrostatic stress, and q is the second deviatoric stress invariant (von Mises stress). d and β are the corresponding Drucker-Prager parameter for cohesion and friction angle, and $\dot{\varepsilon}^{p}_{vol}$ and $\dot{\varepsilon}^{p}_{dev}$ are the volumetric and deviatoric plastic strain-rates. The straight line describes the corresponding Drucker-Prager failure surface (Heinonen, 2004).

NUMERICAL MODEL FOR MONOPILE INTERACTION WITH RIDGE KEEL

Model configuration

The finite element model for a monopile interaction with the ridge keel is shown in Fig. 3. Commercial software Abaqus/Explicit version 2022 was applied for numerical simulations using Coupled Eulerian-Lagrangian (CEL) framework. The shear-cap material model was implemented via user subroutine (VUMAT in Abaqus).

The cylindrical structure was modelled with rigid elements. The ridge-structure interaction process was considered quasi-static, so the dynamic behaviour of the structure could be ignored. Therefore, the structure was described by its shape (cylindrical) and size (diameter). The interaction between the structure and ice was introduced by a general contact algorithm based on Coulomb friction model (friction coefficient 0.1).

The shape of the ridge keel was chosen according to guidelines in ISO 19906 (2019) standard as shown in Fig. 4. Common values from the Gulf of Bothnia were chosen for geometrical dimensions. By utilizing symmetry, only half of 3D ridge geometry was modelled. In the CEL-modelling, the material flows through the finite element mesh. Therefore, the user needs to define a computational domain large enough for the material itself plus necessary additional space for the deformations to avoid boundary effects or material losses from the model as illustrated in Figure 3. In the CEL-model the red colour indicates the region of ice rubble and the blue colour the “empty volume” (without ice).

The ridge width in the horizontal direction perpendicular to ridge motion was modelled large enough to avoid any boundary effects. Eulerian boundary conditions at the far-end surface were given so that theoretically the rubble material can flow in or out of the Eulerian domain freely. Implementing the far-end boundary in this way mitigates the stress waves and prevents the wave mirroring from the model boundary back to the active ice failure zone.

The consolidated layer was introduced as a horizontal Lagrangian contact plane to restrict the up-flow of rubble due to the buoyancy and interaction with the structure. The contact plane was placed at the top of the rubble. The implementation for the consolidated layer was done in this way to introduce realistic boundary conditions at the top of keel rubble without modelling the complicated ice failure processes in the consolidated layer. Therefore, only the rubble part in the keel and its interaction with the monopile was modelled. The sail was ignored, because its load contribution is small compared to the keel load. Main parameters regarding the ridge geometry and material parameters are given in Tables 1 and 2.

The simulation was made in two analysis steps; the first step was used to apply the internal stress state in the keel due to buoyancy. In the second step the monopile structure penetrated with a constant velocity through the ridge. The main output quantities were local contact forces and global resultant forces on the monopile structure, displacements, velocities, and accelerations of each element, and stresses and strains of each element. The failure process was studied by strain fields and void ratio in each ice rubble element.

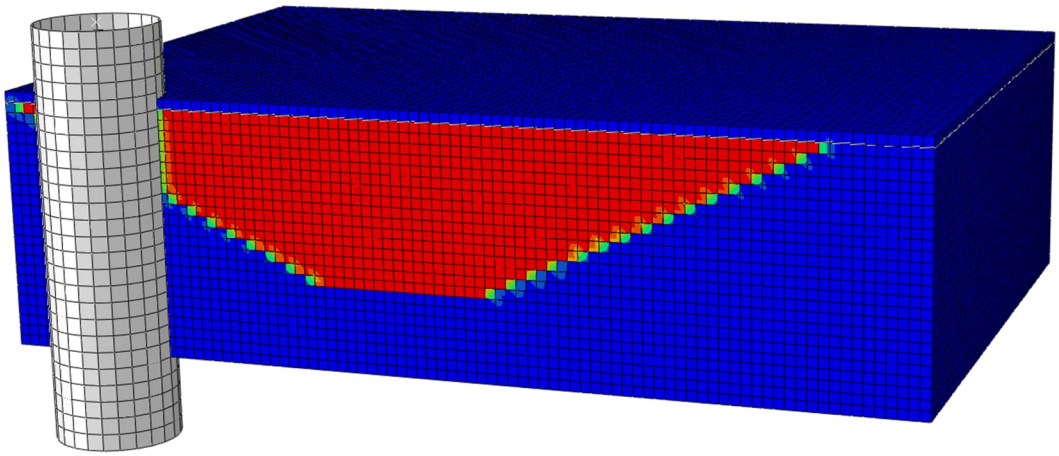

Figure 3. Coupled Eulerian-Lagrangian simulation model of the monopile interaction with the ridge keel. The ridge moves in the direction of the left. Half of 3D geometry was modelled wi th symmetric boundary conditions. The modelled domain consists of two regions: Red colour indicates the initial region of ice rubble, and blue colour indicates the "empty volume" (witho ut ice).

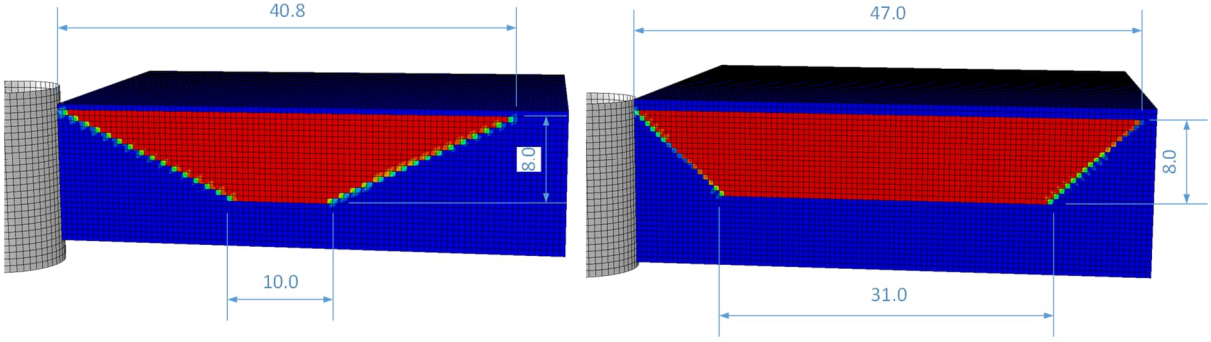

Figure 4. Simulated ridge keel geometries. Left: standard ridge; right: long ridge.

Table 1. Main dimensions in the numerical model: standard ridge and long ridge.

Variable	**Value**
Diameter of the structure	[4, 6, 8, 10, 12] m
Thickness of the keel	8.0 m
Ridge width at the keel top	[40.8, 47.0] m
Ridge width at the keel bottom	[10.0, 31.0] m
Ridge width in the horizontal direction perpendicular to ridge motion	80 m (40 m half-model)

Table 2. Mechanical properties of ice rubble (Heinonen, 2004).

Variable	Symbol	Value	Unit
Density of ice	ρ_i	910	kg/m3
Density of water	ρ_w	1000	kg/m3
Porosity of rubble	η	0.3	[-]
Density of rubble*	ρ_r	937	kg/m3
Elastic modulus	E	1.1	GPa
Poisson value	υ	0.3	[-]
Cohesion	d	5	kPa
Friction angle	β	30	deg
Cap shape factor	R	0.5	[-]
Hydrostatic pressure strength	p_0	8.55d	Pa

*Submerged rubble: $\rho_r = \rho_i(1-\eta) + \rho_w\eta$

Simulation cases

Several simulations were carried out by varying the diameter of the monopile (five diameters) and by varying the ridge keel bottom width (two widths), as shown in Table 3.

Table 3. Simulation cases.

Case	Diameter (m)	Ridge geoemtry
#1	4	Standard
#2	6	Standard
#3	8	Standard
#4	10	Standard
#5	12	Standard
#6	10	Long

RESULTS

The main aspects from the simulations were to analyze the resultant ridge keel forces on the structure and their distribution between parts divided by a horizontal layer positioned at the same level as the initial depth of the keel (-8 m, see Fig. 5). We also analyzed the failure progression in the keel to understand the dominant failure mode and how the failure progression affects the keel load and its changes in the load history.

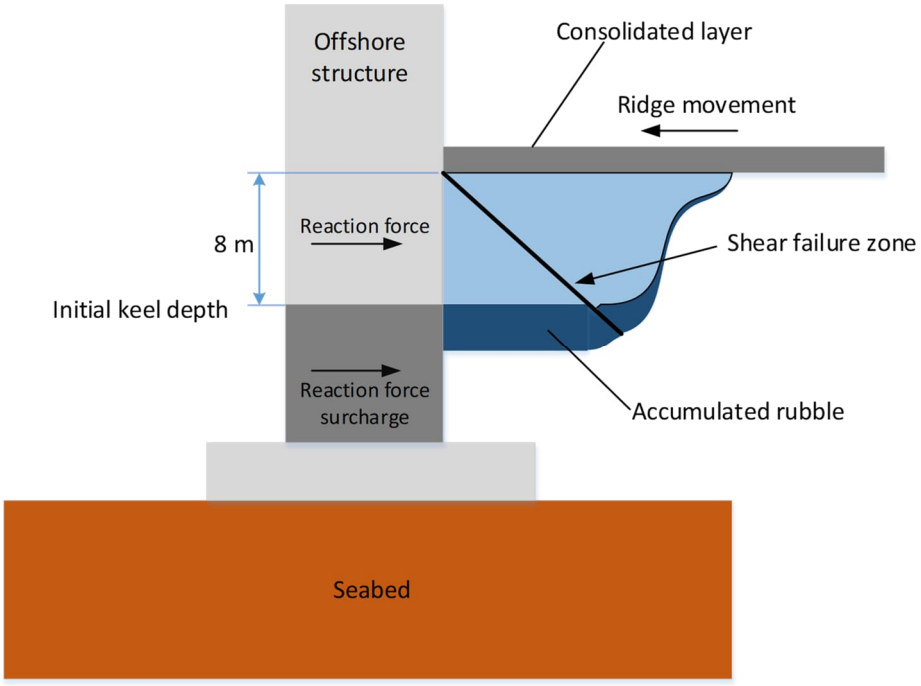

Figure 5. A sketch of keel deformations (coloured in dark blue) and structural parts in which the reaction forces are analyzed.

The failure progression in the keel is shown in by snap-shot pictures from the simulated time histories (Fig. 6). The shear failure is introduced by the equivalent deviatoric plastic strain. An inclined shear failure zone proceeds from the top towards the keel bottom. The wedge-like failure pattern in front of the cylinder takes place first, right after a local force peak (see Fig. 6). Observations from the numerical simulation is in line with previous observations made by other theoretical models as shown in various references (*e.g.* Palmer and Croasdale (2012)). This process was repeated after each load peak, when the keel started to soften due to the shear failure process. As the penetration progressed, the keel became thicker due to the shape of the keel at the front. Therefore, the following local peak forces became higher and higher until the structure reached the position where the keel was thickest. Thereafter, the keel fails by splitting along the symmetry plane in the ice drift direction or by shear plug failure. The splitting happened only with a small diameter (4 m) while the other diameters caused shear plug failure. At this moment, the load collapsed drastically.

The aspect ratio (h_k/w) had some influence also on the load histories: for diameters of 10 and 12 m, the maximum load took place just before the shear plug failure, but for 6 and 8 m, the maximum load occurred at an earlier phase, even though the final keel collapse took place by shear plug failure.

The volumetric changes and relocation of broken ice rubble are introduced by a deformed state (elements in red) in Fig. 7. Even though the structure is relatively slender (the diameter is about the same as the keel depth), some ice accumulation in front of the structure was found at the keel bottom. During the ridge-structure interaction, the ice contact area increases due to keel failure and subsequent broken ice accumulation, as shown in Fig. 7. Even though some of the broken ice rubble is able to flow beside the structure, significant accumulation was observed in all cases. Rubble accumulation is caused by the rubble dilatation (expansion) due to the shear

failure and relocation of broken ice material. The maximum keel thicknesses during the simulations are collected in Table 4. Hence, the ridge keel becomes thicker, but the load increase is minimal (less than 3 % in horizontal directions), as shown in load time history plots in Fig. 8. Corresponding maximum loads are collected in Table 5. The most important change in loads was observed in the vertical direction, because the increased volume of ice rubble induces increased buoyancy. This, together with increased contact area and frictional forces, causes the vertical load increase.

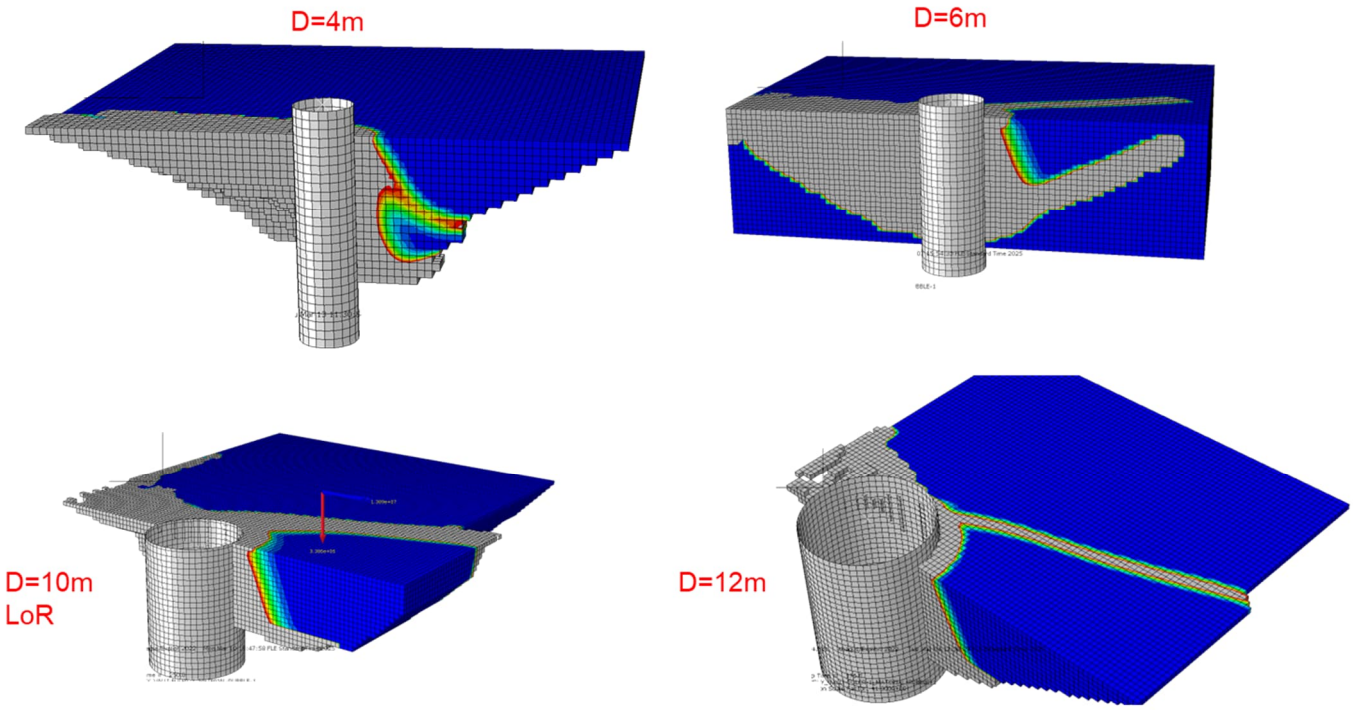

Figure 6. Snap-shot pictures of the shear failure progress in the keel when the ridge moves in the direction of the left. Grey colour indicates localized zones of strains (equivalent deviatoric plastic strains) representing shear failure. The legend “LoR” refers to the long ridge case.

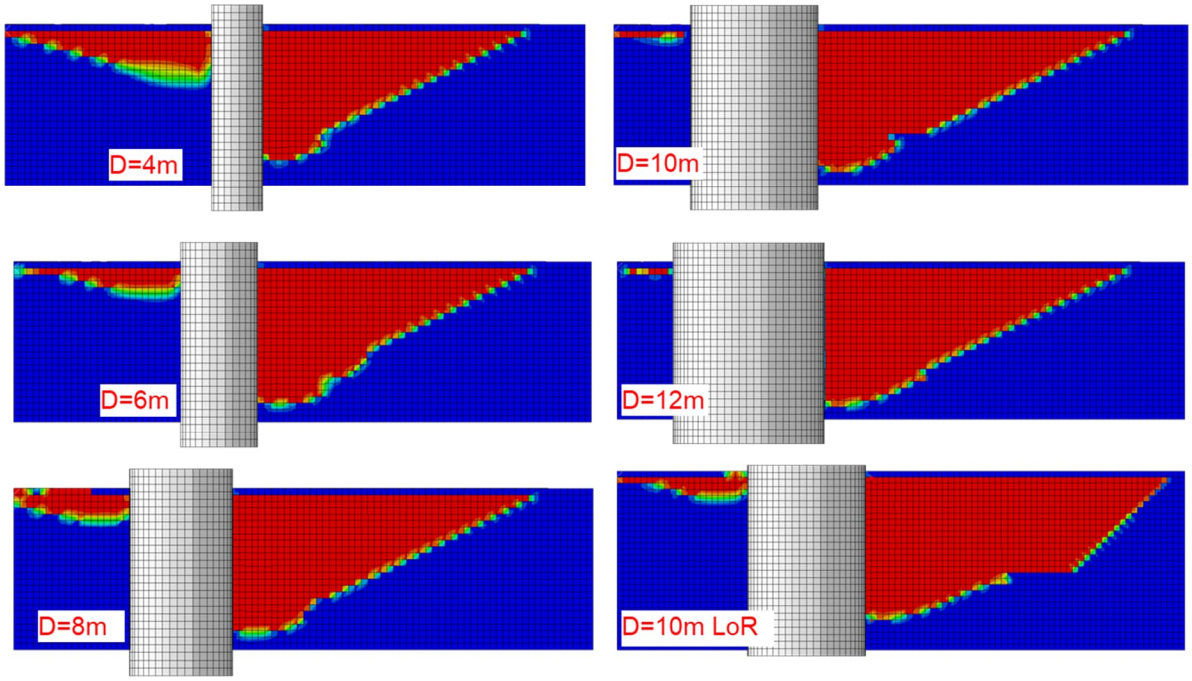

Figure 7. Cross-sectional pictures of the keel deformations from various simulation cases. The selected time instant shows the largest surcharge when the ridge moves in the direction of the left. Red colour indicates the region of ice rubble, while blue represents empty areas (without ice). The legend "LoR" refers to the long ridge case.

Table 4. Maximum keel thickness h_r at the symmetry plane with the corresponding time during the ridge-structure interaction. The intact keel thickness was 8 m. Comparison to Dolgopolov's design thickness: $h_k \leq h_r \leq h_k + w/2$

Diameter (m)	Ridge geometry	t (s)	h_r (m)	h_k (m)	$h_k+w/2$ (m)
4	Standard ridge	172	10.25	8	10
6	Standard ridge	175	10.75	8	11
8	Standard ridge	170	10.75	8	12
10	Standard ridge	160	11.25	8	13
12	Standard ridge	148	11.25	8	14
10	Long ridge	210	12.25	8	13

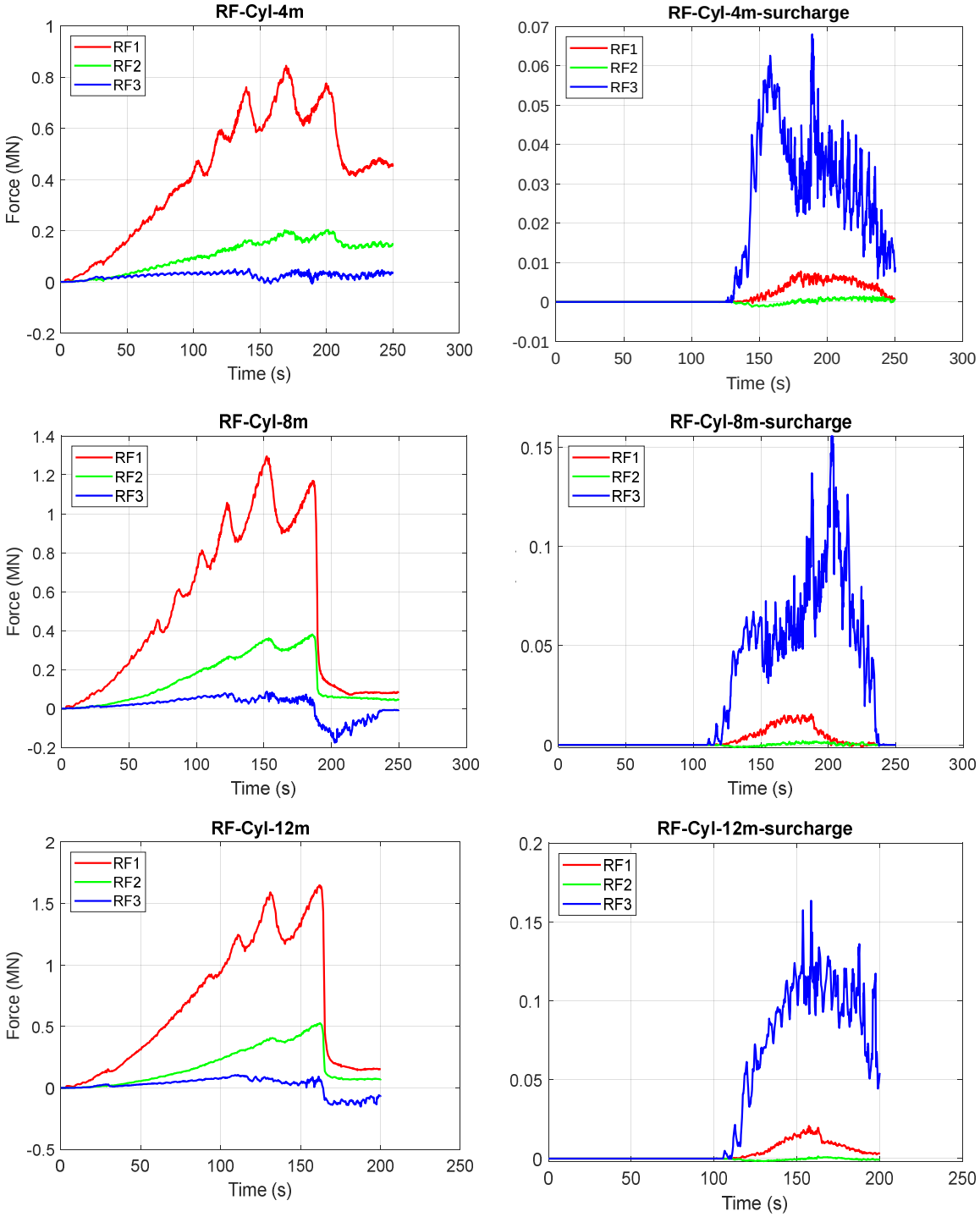

Figure 8. Simulated force time history plot of the global keel load (MN) on the structure in three main directions. RF1in the ice drift direction, RF2 in the transversal direction (only the symmetric half-model) and RF3 in the vertical direction. Right-hand side plots represent the loads on the lower part of the monopile (surcharge, below the intact keel bottom at 8 m). Three simulation cases from top to bottom: diameters 4 m, 8 m and 12 m.

Table 5. Maximum global keel loads in three main directions. RF1 in ice the drift direction, RF2 in the transversal direction and RF3 in the vertical direction. The columns for surcharge represent the loads on the lower part of the monopile (below the intact keel bottom at 8 m). The legend "LoR" refers to the long ridge case.

				Surcharce		
Diameter (m)	RF1 (MN)	RF2 (MN)	RF3 (MN)	RF1 (MN)	RF2 (MN)	RF3 (MN)
4	0.844	0.203	0.051	0.008	0.001	0.068
6	1.065	0.276	0.056	0.014	0.003	0.180
8	1.295	0.381	0.088	0.015	0.002	0.156
10	1.492	0.450	0.084	0.019	0.003	0.306
12	1.648	0.526	0.105	0.021	0.001	0.163
10 "LoR"	1.680	0.536	0.078	0.032	0.009	0.242

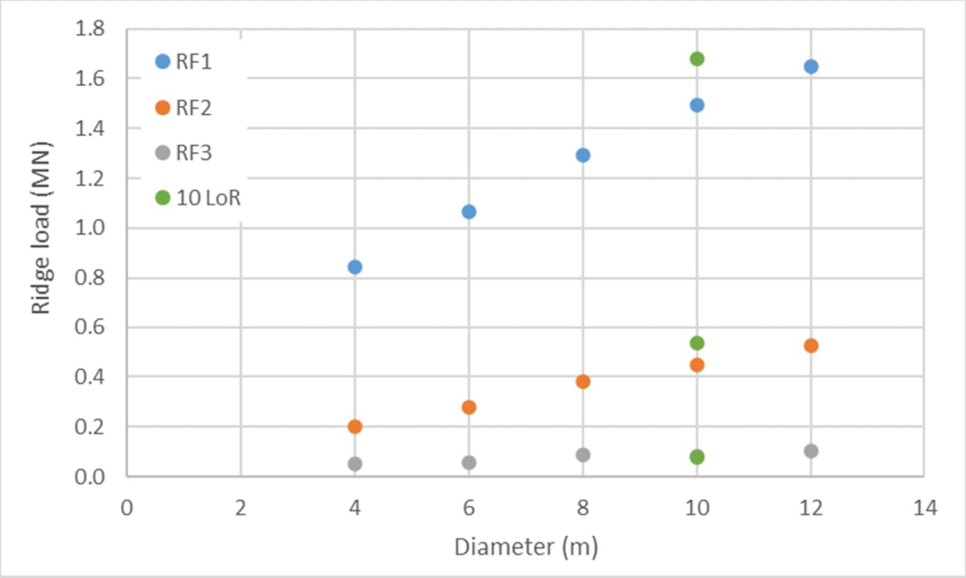

Figure 9. Maximum global keel loads in three main directions RF1 in the ice drift direction, RF2 in the transversal direction and RF3 in the vertical direction, Additional dots for the diameter of 10 m represent the loads from the long ridge case, while the rest are for the standard ridge.

The global ridge loads show that for all load components, the maximum loads increase as the diameter of the structure increases (see Fig. 9). It is also noteworthy that the length of the ridge keel in the direction of ice drift influences the loads. A longer keel induces larger loads.

CONCLUSIONS

During the ridge-structure interaction, ice rubble first fails locally in contact with the cylindrical structure. Subsequently, the keel thickness increases in front of the structure, but the accumulated volume is mostly caused by broken ice mass. Even though the contact area of the keel increases, the accumulated mass of ice rubble has only frictional resistance and therefore cannot transmit significant load on the structure. Consequently, the surcharge effect for narrow-like structures was observed to be minimal.

Dolgopolov's model describes the local keel failure in front of the structure (wedge-like failure pattern). The determination of ridge load using Dolgopolov's model does not include effects from ridge geometry other than the thickness of the keel. However, the simulations showed that the length of ridge in the ice drift direction is an important factor. For selected ridge geometries, the shear plug failure limited the maximum load when the diameter was greater than 4 m. For the narrowest structure (diameter = 4 m), the ridge split in the ice drift direction along the symmetry plane.

Our main statements are the following:

- Ice rubble accumulates in front of the structure roughly as suggested by Dolgopolov *et al.* (1975)
- The load increase is small and does not increase as suggested by Dolgopolov *et al.* (1975)
- The ridge geometry and size matter, and the maximum keel load is the minimum of the two failure modes: Dolgopolov's wedge-like failure and the global keel failure (shear plug failure)
- More research is needed to clarify the effect of the size and geometry of both the ridge and the structure.

ACKNOWLEDGEMENTS

The authors gratefully acknowledge the following funders: Terramare-Boskalis, Labkotec Oy, Skarta Energy Oy, Skyborn Renewables AB, OX2, Metsähallitus, and Aker Arctic for funding the SBP-IceWind project; the Academy of Finland for funding the WindySea project (Special RRF funding for research on key areas of green and digital transition [grant number 348588]); and the RePower project funded by the European Union NextGenerationEU. The RePower project is part of the strategic research opening "Electric Storage" of VTT, launched with the support of the additional chapter of the RePowerEU investment and reform programme for sustainable growth in Finland. Finally, we would like to acknowledge also the IceWise project (352996) supported by the Research Council of Norway and the IceWise partners.

REFERENCES

Dolgopolov, YU, Afanasiev, VP, Koren'Kov, VA, Panfilov, DF. 1975. Effect of Hummocked Ice on the Piers of Marine Hydraulic Structures, International Symposium on Ice Problems, 3rd, Proceedings, Dartmouth College, Hanover, NH. Aug., 18-21. 1975., p. 469-477

Heinonen, J., Constitutive Modeling of Ice Rubble in First-Year Ridge Keel, VTT Publications 536, Espoo 2004, 142 p., Doctoral thesis, ISBN 951-38-6930-5 (sort back ed.), URL: http://www.vtt.fi/inf/pdf/publications/2004/P536.pdf

Heinonen, J. 2022, Ridge Load on the Monopile: A Comparison Between FEM-CEL–Simulations and ISO 19906. in J Tuhkuri & A Polojärvi (eds), IUTAM Bookseries. Springer, IUTAM Bookseries, vol. 39, pp. 227-239, IUTAM Symposium on Physics and Mechanics of Sea Ice, Espoo, Finland, 3/06/19. https://doi.org/10.1007/978-3-030-80439-8_11

Heinonen, J. Tikanmäki, M., Mikkola, E., Perälä, I., Shestov, A., Høyland, K.V., Salganik E., van den Berg, M., Li, H., Jiang, Z., Ervik, Å., Puolakka, O. 2021. Scale-model ridges and interaction with narrow structures, Part 3 Analysis of Ridge Keel Punch Tests, *Proceedings of the 26th International Conference on Port and Ocean Engineering under Arctic Conditions*, June 14-18, 2021, Moscow, Russia

ISO 19906, 2019. Petroleum and natural gas industries - arctic offshore structures, second edition, International Organization for Standardization, Geneva, Switzerland".

Jiang, Z., Heinonen, J. Tikanmäki, M., Mikkola, E., Perälä, I., Shestov, A., Høyland, K.V., Salganik E., van den Berg, M., Li, H., Ervik, Å., Puolakka, O. 2021. Scale-model ridges and interaction with narrow structures, Part 4 Global loads and failure mechanisms, *Proceedings of the 26th International Conference on Port and Ocean Engineering under Arctic Conditions*, June 14-18, 2021, Moscow, Russia

Jiang, Z. 2020. Experimental investigation of ice loads on vertical and slope offshore structures, Thesis for the degree of Master of Science at the Norwegian University of Science and Technology (NTNU) and Aalto University.

Kärna T. and Nykänen, E (2004). An approach for ridge load determination in probabilistic design. Proc. of the 17th Int. Symp. on Ice (IAHR), St. Peterburg, Russia, 2: pp. 42-50.

Palmer, A and Croasdale K. 2012. Arctic Offshore Engineering, World Scientific Publishing Company, 2012. Singapore. eBook ISBN 9789814368780

Salganik E., Ervik, Å., Heinonen, J. Høyland, K.V., Perälä, I., Puolakka, O., Shestov, A., van den Berg, M. 2021. Scale-model ridges and interaction with narrow structures, Part2: thermodynamics of ethanol ice. *Proceedings of the 26th International Conference on Port and Ocean Engineering under Arctic Conditions*, June 14-18, 2021, Moscow, Russia

Serré, N., Liferov, P., 2010. Loads from ice ridge keels - experimental vs. numerical vs. analytical. In: *Proc. of the 20 Int. Symp. on Ice (IAHR), 2010, Lahti, Finland*. Paper # 92

Shestov, A., Ervik, Å., Heinonen, J., Perälä, I., Høyland, K.V., Salganik E., Li, H., van den Berg, M., Jiang, Z., Puolakka, O. 2020. Scale model ridges and interaction with narrow structures, Part 1 Overview and scaling. *25th IAHR International Symposium on Ice, Trondheim, Norway*